Dalton Transactions

PAPER

View Article Online
View Journal | View Issue

Cite this: *Dalton Trans.*, 2016, **45**, 9860

Structurally versatile phosphine and amine donors constructed from N-heterocyclic olefin units†

Nathan R. Paisley,‡ Melanie W. Lui,‡ Robert McDonald, Michael J. Ferguson and Eric Rivard*

Received 21st January 2016,
Accepted 17th February 2016

DOI: 10.1039/c6dt00299d

www.rsc.org/dalton

A general strategy for the synthesis of hindered N- and P-based donors is presented whereby the strongly electron releasing N-heterocyclic olefin (NHO) unit, IPr=CH–, (IPr=CH– = $[(HCNDipp)_2C{=}CH]^-$; Dipp = 3,6-$^i Pr_2C_6H_2$) is linked to terminally bound phosphine and amine donors. Preliminary coordination chemistry is presented involving phosphine (IPr=CH)PR_2 (R = ^{i}Pr and Ph) and amine (IPr=CH)NMe_2 ligands and the Lewis acids BH_3 and AuCl. Interestingly, (IPr=CH)NMe_2 binds AuCl through an exocyclic olefin unit, while the softer phosphorus centers in (IPr=CH)PR_2 coordinate to yield Au–P linkages; thus the reported NHO-based ligands exhibit tunable binding modes to metals.

Introduction

Sterically encumbered phosphines and N-heterocyclic carbenes (NHCs) are effective ligands for supporting a variety of catalytic bond-forming processes,[1] and can stabilize highly reactive molecular entities *via* strong coordinative interactions.[2] Common traits between these two ligand classes are the presence of a strongly σ-donating atom, ease of synthesis, and a high level of structural tunability. A related ligand group that is attracting increasing attention of late are N-heterocyclic olefins (NHOs),[3] which contain considerable nucleophilic character due to the highly polarized nature of the exocyclic C=C double bond, allowing these species to be strong neutral 2-electron donors (Chart 1; left). Accordingly, NHOs are now being used to intercept reactive inorganic species,[4,5] as organocatalysts for various polymerization strategies,[6] and as a component of pincer-type ligands.[7]

In this paper, we present efficient routes to phosphine and amine donors that contain an NHO moiety $[IPr{=}CH]^-$ directly linked to P- and N-donor sites. As shown in Chart 2, there is a possibility of coordination through either the NHO (*via* carbon-ligation) or the terminal P/N atoms. Our current study was motivated in part by the prior work of Beller who demonstrated that imidazolium-alkylphosphines (Chart 1; right) when combined with Pd(II) sources and base, afforded active catalysts (*in situ*) for the hydroxylation of arylhalides, and for both C–N (Buchwald–Hartwig) and C–C (Sonogashira) coupling reactions.[8] Despite the possible formation of neutral NHO-linked phosphines (NHOPs; Chart 2; E = P) during Beller's catalytic processes, such ligands were not isolated, nor were any well-defined metal complexes with these ligands reported. As a result, we decided to explore this ligand class in more detail and consequently uncovered divergent coordination behavior towards AuCl, depending if hard amine- or soft-phosphine groups are appended to an NHO unit.

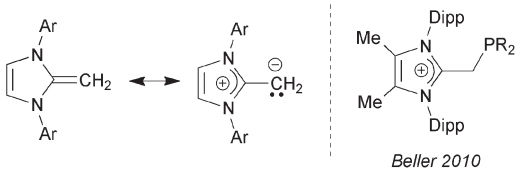

Chart 1 (Left) Canonical forms for a generic N-heterocyclic olefin (NHO); (Right) Beller's imidazolium alkylphosphines; Ar = aryl; Dipp = 2,6-$^i Pr_2C_6H_3$.

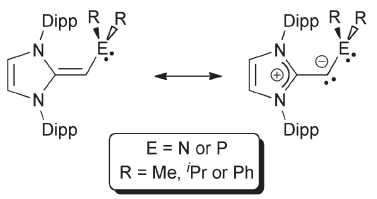

Chart 2 N-Heterocyclic olefin-phosphines (NHOP) or -amines (NHON) discussed in this paper.

Department of Chemistry, University of Alberta 11227 Saskatchewan Drive, Edmonton, AB, T6G 2G2 Canada. E-mail: erivard@ualberta.ca

†Electronic supplementary information (ESI) available: NMR spectra for all compounds and refined structure of **11**. CCDC 1448842–1448851. For ESI and crystallographic data in CIF or other electronic format see DOI: 10.1039/c6dt00299d

‡These authors contributed equally to this study.

Results and discussion

Synthesis of N-heterocyclic olefin phosphines (NHOPs)

We began our studies by exploring the synthesis of the diisopropylphosphine-capped N-heterocyclic olefin (IPr=CH)P^{i}Pr$_2$ **2** (IPr = [(HCNDipp)$_2$C]; Dipp = 2,6-^{i}Pr$_2$C$_6$H$_3$). In line with prior work from our group,[9] the readily available NHO, IPr=CH$_2$ **1**,[3d] was combined with ClP^{i}Pr$_2$ in a 1 : 1 ratio in THF (Scheme 1) with the intention of first isolating the imidazolium salt [IPr-CH$_2$-P^{i}Pr$_2$]Cl, which would be isostructural to Beller's pre-ligands shown in Chart 1. While there was spectroscopic evidence for the formation of the desired imidazolium salt, the starting material IPr=CH$_2$ **1** was sufficiently basic to deprotonate [IPr-CH$_2$-P^{i}Pr$_2$]Cl to give **2** and the known by-product [IPrCH$_3$]Cl.[9] Fortunately **2** and [IPrCH$_3$]Cl have quite different solubilities, allowing for their easy separation. By altering the ratio between IPr=CH$_2$ **1** and ClP^{i}Pr$_2$ to 2 : 1 (eqn (1)) and conducting the reaction in THF at room temperature for 20 h, we were able to isolate pure (IPr=CH)P^{i}Pr$_2$ **2** in 81% yield after extracting **2** from the product mixture (containing [IPrCH$_3$]Cl) with hexanes. Following a similar procedure, the phenyl-substituted NHOP (IPr=CH)PPh$_2$ **3** was prepared in an isolated yield of 83% (eqn (1)). The new NHOPs **2** and **3** were each characterized by NMR spectroscopy, elemental analysis and X-ray crystallography (colorless crystals grown from hexanes at −30 °C; Fig. 1 and 2).

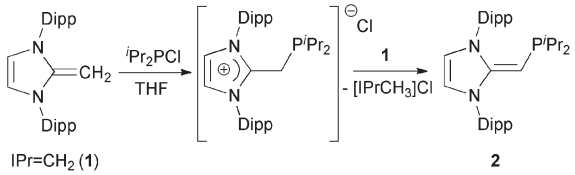

Scheme 1 In the reaction of IPr=CH$_2$ (**1**) and ^{i}Pr$_2$PCl in a 1 : 1 ratio, we observe the formation of the imidazolium-alkylphosphine salt [IPr-CH$_2$-P^{i}Pr$_2$]Cl as well as the desired neutral NHO-appended phosphine **2**.

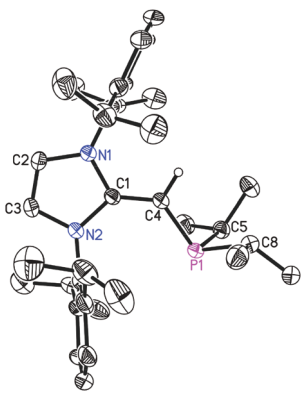

Fig. 1 . Molecular structure of **2** with thermal ellipsoids at the 30% probability level. Only one of the four crystallographically-independent molecules in the unit cell is presented. The hydrogen atom attached to C(4) is shown with an arbitrarily small thermal parameter; all other hydrogen atoms have been omitted for clarity. Selected bond lengths (Å) and angles (°): P–C(4) 1.780(3)–1.788(3), P–C(5) 1.835(4)–1.883(3), P–C(8) 1.859(4)–1.896(4), C(1)–C(4) 1.364(4)–1.366(4); P–C(4)–C(1) 126.9(2)–129.8(2), N(1)–C(1)–N(2) 104.0(2), C(4)–P–C(5) 101.03(14)–105.72(18), C(4)–P–C(8) 99.71(15)–104.29(17), C(5)–P–C(8) 99.12(14)–101.57(17).

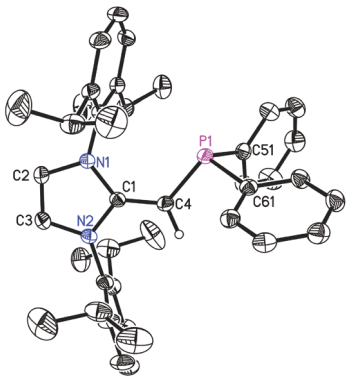

Fig. 2 Molecular structure of **3** with thermal ellipsoids at the 30% probability level. The hydrogen atom attached to C(4) is shown with an arbitrarily small thermal parameter; all other hydrogen atoms have been omitted for clarity. Selected bond lengths (Å) and angles (°) with values corresponding to a second molecule in the asymmetric unit in square brackets: P(1)–C(4) 1.7762(15) [1.782(2)], P(1)–C(51) 1.8411(16) [1.839(2)], P(1)–C(61) 1.8406(15) [1.8448(18)], C(1)–C(4) 1.365(2) [1.377(2)]; C(4)–P(1)–C(51) 104.37(7) [104.50(9)], C(4)–P(1)–C(61) 99.75(6) [99.70(8)], P(1)–C(4)–C(1) 126.25(11) [126.16(16)], N(1)–C(2)–N(2) 104.08(12) [104.29(12)].

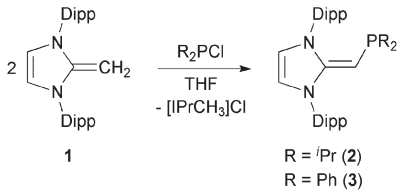

(1)

The refined structure of (IPr=CH)P^{i}Pr$_2$ **2** is presented in Fig. 1 with only one of the four crystallographically-independent molecules in the unit cell shown; thus, selected bond lengths and angles are provided as a range. The exocyclic C=C bonds in **2** [C(1)–C(4) = 1.364(4) to 1.366(4) Å] are considerably shorter than the typical C–C single bond length of *ca.* 1.530 Å,[10] and is only slightly elongated compared to the exocyclic C=C bond length of 1.332(4) Å in free IPr=CH$_2$.[3c] As expected, the crystallographically determined C(sp^2)–P linkages in **2** [C(4)–P(1) = 1.780(3) to 1.788(2) Å] are contracted with respect to the C(sp^3)–P bonds involving the ^{i}Pr substituents [1.835(4) to 1.896(4) Å]. For comparison the C(olefin)–P distances in *cis*-Ph$_2$P–CH=CH–PPh$_2$ are 1.817(3) and 1.825(3) Å,[11] suggesting a possible increase in C(π) → P–C(σ^*) hyperconjugation in **2**, leading to shorter C(sp^2)–P bonds. The overall metrical parameters in (IPr=CH)PPh$_2$ (**3**) (Fig. 2) are quite similar to that of **2** with an average C(4)–P(1) distance of 1.780(2) Å in **3** and average C(1)–C(4)–P(1) angles of 126.0(2)°, compared to a range of 126.9(2) to 129.8(2)° in **2**.

Synthesis of the N-heterocyclic olefin amine (IPr=CH)NMe_2 4

In addition to preparing NHOPs, we wanted to see if a harder amine donor could be incorporated onto an NHO scaffold. The dimethylamino-substituted NHO, (IPr=CH)NMe_2 **4**, was prepared by combining two equivalents of the commercially available carbene IPr with one equivalent of Eschenmoser's salt $[H_2C{=}NMe_2]I$[12] in toluene (eqn (2)). In this process, the first equivalent of IPr is believed to undergo a nucleophilic attack on the iminium moiety to form [IPr-CH_2–NMe_2]I which is then subsequently deprotonated by a second equivalent of IPr to yield (IPr=CH)NMe_2 **4** and the imidazolium by-product [IPrH]I (which can be recycled for the preparation of IPr) (eqn (2)). In a similar fashion as the syntheses of **2** and **3**, the salt by-product [IPrH]I is much less soluble than the target ligand **4**, thus separation could be achieved by filtering the reaction mixture. One drawback with this synthesis is that the crude samples of **4** occasionally contains *ca.* 5–10% of unreacted IPr (as determined by ^{1}H NMR), which is difficult to separate from (IPr=CH)NMe_2 **4** due to their similar solubilities in common organic solvents. However, a successful way to remove the IPr contaminant involves adding a small amount of BPh_3 to form the known adduct IPr·BPh_3,[13] which is much less soluble in hexanes than **4**.

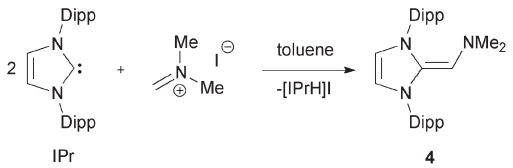

(2)

The structure of (IPr=CH)NMe_2 **4** was authenticated by X-ray crystallography (Fig. 3) and this study revealed an exocyclic C(1)–C(4) bond length of 1.3463(14) Å which is slightly shorter than the corresponding distances in the NHOPs **2** and **3**, suggesting the retention of substantial C–C π-bonding in this unit. The C(1)–C(4)–N(1) angle was also consistent with sp^2-hybridization at C(4) [122.98(9)°], while the nitrogen atom of the –NMe_2 group is significantly pyramidalized [$\Sigma°$(N) = 333.35(17)°] consistent with a lack of substantial N(3)–C(4) π-bonding.

Coordination of the NHOPs 2 and 3 to BH_3 and AuCl

With the new NHOPs in hand, we first tested their reactivity with the Lewis acid source THF·BH_3. When either (IPr=CH)-P^iPr_2 **2** or (IPr=CH)PPh_2 **3** was combined with THF·BH_3 in hexanes (eqn (3)), the reaction mixture went from yellow to colorless after 90 min at room temperature. After the volatiles were removed, the respective phosphine–borane adducts (IPr=CH)$^iPr_2P{\cdot}BH_3$ **5** and (IPr=CH)$Ph_2P{\cdot}BH_3$ **6** were isolated as colorless crystals in 52 and 56% yields after recrystallization from cold (−30 °C) hexanes or toluene (slow evaporation), respectively. As expected, coordination of a BH_3 unit was evident by NMR spectroscopy, which showed broad ^{11}B NMR resonances at −42.0 and −35.8 ppm for **5** and **6**, respectively, consistent with the presence of four-coordinate boron environments. In addition, considerable downfield shifts in the ^{31}P resonances were noted within the NHOPs upon BH_3 coordination: from −17.4 ppm in **2** to 21.9 ppm in (IPr=CH)$^iPr_2P{\cdot}BH_3$ **5**; from −31.4 ppm in **3** to 7.3 ppm in (IPr=CH)-$Ph_2P{\cdot}BH_3$ **6**. Such a substantial change in ^{31}P NMR chemical shift indicated the likely presence of BH_3 units bound to the phosphorus centers; this postulate was confirmed by performing single-crystal X-ray crystallography (**5**: Fig. 4; **6**: Fig. 5).

As shown in Fig. 4, (IPr=CH)$^iPr_2P{\cdot}BH_3$ **5** contains a P-bound borane residue with a P–B bond length of 1.9166(18) Å; for comparison, the dialkylphosphine–borane adduct $^tBu_2PH{\cdot}BH_3$ has a P–B bond length of 1.936(2) Å.[14] In the case of (IPr=CH)$^iPr_2P{\cdot}BH_3$ **5**, the P(1)–C(4) length [1.7504(14) Å] is contracted in comparison to the corresponding distance in the free phosphine (IPr=CH)P^iPr_2 **2** [1.780(3) to 1.788(2) Å]. The

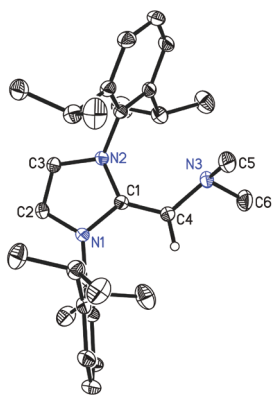

Fig. 3 Molecular structure of **4** with thermal ellipsoids at the 30% probability level. The hydrogen atom attached to C(4) is shown with an arbitrarily small thermal parameter; all other hydrogen atoms have been omitted for clarity. Selected bond lengths (Å) and angles (°): N(1)–C(1) 1.4024(12), N(2)–C(1) 1.4009(12), C(1)–C(4) 1.3463(14), C(4)–N(3) 1.4299(13), N(3)–C(5) 1.4563(16), N(3)–C(6) 1.4570(16); N(1)–C(1)–N(2) 104.44(8), N(1)–C(1)–C(4) 125.71(9), C(1)–C(4)–N(3) 122.98(9), C(4)–N(3)–C(6) 110.19(10).

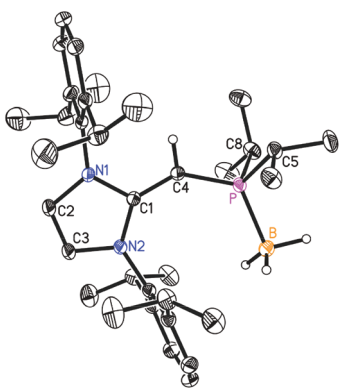

Fig. 4 Molecular structure of **5** with thermal ellipsoids at the 30% probability level. The hydrogen atom attached to C(4) is shown with an arbitrarily small thermal parameter; all other hydrogen atoms have been omitted for clarity. Selected bond lengths (Å) and angles (°): P–B 1.9166(18), P–C(4) 1.7504(14), C(1)–C(4) 1.3749(18), P–C(5) 1.8486(14), P–C(8) 1.8495(16); C(4)–P–B 124.56(7), P–C(4)–C(1) 138.02(11), C(4)–P–C(5) 102.07(7), C(4)–P–C(8) 106.76(7), B–P–C(5) 110.56(8), B–P–C(8) 107.50(8).

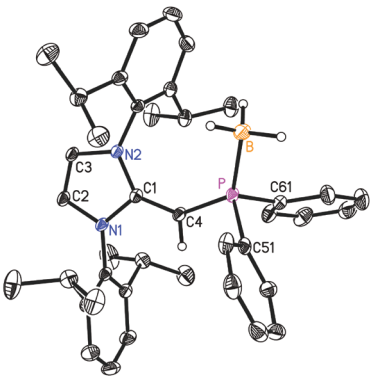

Fig. 5 Molecular structure of **6** with thermal ellipsoids at the 30% probability level. The hydrogen atom attached to C(4) is shown with an arbitrarily small thermal parameter; all other hydrogens have been omitted for clarity. Selected bond lengths (Å) and angles (°): P–B 1.9242(18), P–C(4) 1.7479(11), C(1)–C(4) 1.3811(15), P–C(51) 1.8292(12), P–C(61) 1.8300(13); C(4)–P–B 125.76(6), P–C(4)–C(1) 138.31(9), C(4)–P–C(51) 101.10(5), C(4)–P–C(61) 107.67(6), B–P–C(51) 109.21(7), B–P–C(61) 108.15(7).

exocyclic C(1)–C(4) double bond within the NHO unit in **5** [1.3749(18) Å] is essentially the same length within experimental error as the exocyclic C=C bond distances in the phosphine **2** [1.364(4) to 1.366(4) Å]. The main structural change noted upon coordination of BH_3 is a widening of the P–C(4)–C(1) from 126.9(2)° in the free ligand **2** to 138.02(11)° in adduct **5**. Similarly, the P–C(4)–C(1) angle in the phenyl analogue (IPr=CH)Ph_2P·BH_3 (**6**) [138.31(9)°] (Fig. 5) is wider than in the free phosphine (IPr=CH)PPh_2 (**3**) [126.0(2)° *avg.*]. In both compounds **5** and **6**, the BH_3 unit is oriented in an *anti*-fashion with respect to the exocyclic olefinic C–H group, placing the BH_3 group in close proximity to one of the flanking Dipp aryl groups of the NHO ligand; such a coordination mode could enhance aryl···metal interactions within NHOP–metal complexes.[1e]

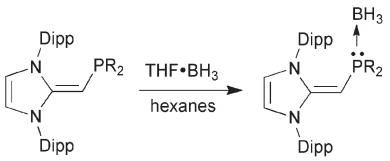

(3)

After demonstrating the successful coordination of the small Lewis acid BH_3 to the NHOPs **2** and **3**, we decided to expand our studies to include transition metals. Our initial explorations focused on the noble metals Pd and Pt since complexes bearing these elements in conjunction with bulky phosphines[15] and NHCs[16] are often used in metal-mediated cross-coupling reactions. Despite the presence of a potentially strongly coordinating terminal –P^iPr_2 unit in (IPr=CH)P^iPr_2 **2**, no discernable reaction was noted when excess **2** (2–3 equiv.) was combined with either $Pd(PPh_3)_4$ or $Pt(PPh_3)_4$ in hot C_6D_6 (50 °C) for 4 days (monitored by ^{31}P NMR spectroscopy). A similar lack of reactivity was found with the two coordinate Pt(0) complex $Pt(P^tBu_3)_2$. Attempts to form a bis NHOP–$PdCl_2$ pre-catalyst[17] by treating $PdCl_2(NCPh)_2$ with two equiv. of **2** in toluene, led to an immediate color change of the reaction mixture from yellow to dark red, however ^{31}P NMR analysis revealed the formation of six spectroscopically distinct products from which a single clean product could not be isolated.

Reports of using $[PdCl(cinnamyl)]_2$ (cinnamyl = η^3-$H_2CCHCH(Ph)$) as a palladium source to generate active L·Pd(cinnamyl) pre-catalysts (L = ligand)[18] in cross-coupling reactions led us to combine $[PdCl(cinnamyl)]_2$ with (IPr=CH)P^iPr_2 **2**. When **2** was mixed with $[PdCl(cinnamyl)]_2$ in toluene several new species were found by ^{31}P NMR spectroscopy. In one case, layering of the crude reaction mixture with hexanes, followed by cooling to −30 °C gave a small batch of yellow crystals (2–3 mg) that were identified by X-ray crystallography as the target Pd(II) complex (IPr=CH)P^iPr_2·PdCl(cinnamyl) **7** (Fig. 6).

Upon closer inspection of the structure of **7** (Fig. 6) it is clear that the –P^iPr_2 unit is free to rotate with respect to the bulky IPr=CH– group. In the BH_3 adduct **5**, the isopropropyl groups are rotated away from the IPr unit, while in (IPr=CH)P^iPr_2·PdCl(cinnamyl) **7** the phosphorus bound ^{i}Pr substituents are positioned toward one Dipp group, enabling the more hindered PdCl(cinnamyl) array to occupy a more open side of the NHOP ligand coordination sphere. Therefore despite the bulk of (IPr=CH)P^iPr_2, there exists sufficient torsional flexibility to allow different coordination pockets to be formed (a useful property for catalysis when various intermediates need to be stabilized). The Pd–cinnamyl bonding interactions in **7** range from 2.113(6) Å to 2.261(5) Å with the longest Pd–C bond to C(53) positioned *trans* to the phosphine donor. In the NHC complex IPr·PdCl(cinnamyl), the related *trans*-positioned Pd–C bond length (with respect to the IPr donor) is 2.201(17) Å,[19] indicating that the ligand (IPr=CH)P^iPr_2 exerts a similar degree of *trans*-influence as IPr.

Given the difficulties faced in introducing an NHOP as a ligand to Pd and Pt centers, we decided the explore the coordi-

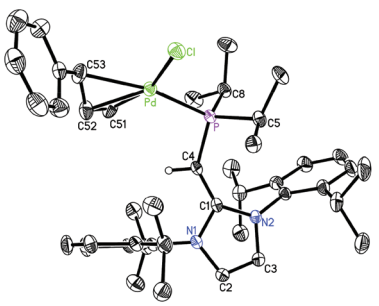

Fig. 6 Molecular structure of (IPr=CH)P^iPr_2·PdCl(cinnamyl) **7** with thermal ellipsoids at the 30% probability level. The hydrogen atom attached to C(4) is shown with an arbitrarily small thermal parameter; all other hydrogens have been omitted for clarity. Selected bond lengths (Å) and angles (°): Pd–P 2.3086(12), Pd–Cl 2.3582(12), Pd–C(51) 2.113(6), Pd–C(52) 2.143(5), Pd–C(53) 2.261(5), P–C(4) 1.765(4), C(1)–C(4) 1.386(6), P–C(5) 1.847(5), P–C(8) 1.863(5); P–Pd–Cl 102.23(4), C(4)–P–Pd 103.85(15), P–C(4)–C(1) 136.1(3), C(4)–P–C(5) 105.8(2), C(4)–P–C(8) 110.7(2), Pd–P–C(5) 117.51(16), Pd–P–C(8) 113.69(18), C(51)–C(52)–C(53) 120.4(6).

nation of this ligand class to gold(I) centers. Added motivation for this work stems from the rapidly growing use of Au(I) complexes in catalysis (*e.g.* in the hydroamination of alkynes).[20] A toluene solution of (IPr=CH)P^{i}Pr$_2$ **2** was added to a molar equivalent of Me$_2$S·AuCl, and after stirring at room temperature for 2 h, (IPr=CH)^{i}Pr$_2$P·AuCl **8** was obtained as a pale yellow solid in an 85% yield after filtration of the reaction mixture and removal of the volatiles (eqn (4)); the resulting product was analytically pure as judged by satisfactory C, H and N analyses. Compound **8** was characterized by X-ray crystallography and the refined molecular structure is shown in Fig. 7. The metrical parameters within the IPr=CH– unit in **8** are similar to those in the BH$_3$ adduct (IPr=CH)^{i}Pr$_2$P·BH$_3$ **5**, with comparable P–C(4) and exocyclic C(1)–C(4) bond lengths [1.7742(19) and 1.376(3) Å, respectively]. Interestingly, the –P^{i}Pr$_2$ unit in **8** is rotated in such as fashion as to place the hindered isopropyl groups away from the Dipp groups within the IPr=CH– unit; as a result the Au(I) center lies over the π-face of a Dipp substituent (Au···C(*ipso*) distance = 3.507 Å), and accordingly the P–Au–Cl angle [171.40(2)°] is distorted from the expected linear geometry. For comparison, shorter arene···Au(I) interactions have been noted within a series of Buchwald biarylphosphine–Au(I) complexes L·Au(NCMe)$^+$ (3.04–3.19 Å).[21] The corresponding diphenylphosphine-capped NHO complex (IPr=CH)PPh$_2$·AuCl **9** was prepared (98% yield) in a similar straightforward manner as **8**, and exhibited the same overall geometry as in **8** (Fig. 8) with a slightly narrower P–Au–Cl angle of 168.72(4)°.

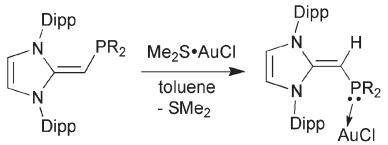

R = ^{i}Pr (**2**)
R = Ph (**3**)

R = ^{i}Pr (**8**)
R = Ph (**9**) (4)

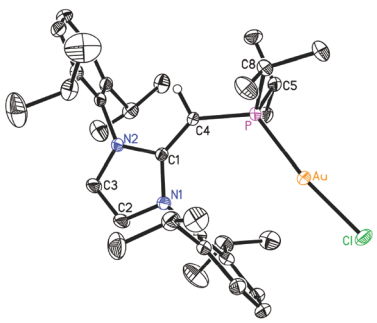

Fig. 7 Molecular structure of **8** with thermal ellipsoids at the 30% probability level. The hydrogen atom attached to C(4) is shown with an arbitrarily small thermal parameter; all other hydrogen atoms have been omitted for clarity. Selected bond lengths (Å) and angles (°): Au–P 2.2348(5), Au–Cl 2.2991(5), P–C(4) 1.7442(19), C(1)–C(4) 1.376(3), P–C(5) 1.848(2), P–C(8) 1.845(2); P–Au–Cl 171.40(2), C(4)–P–Au 122.82(7), P–C(4)–C(1) 136.20(15), C(4)–P–C(5) 105.69(10), C(4)–P–C(8) 104.31(10), Au–P–C(5) 106.89(7), Au–P–C(8) 110.83(7).

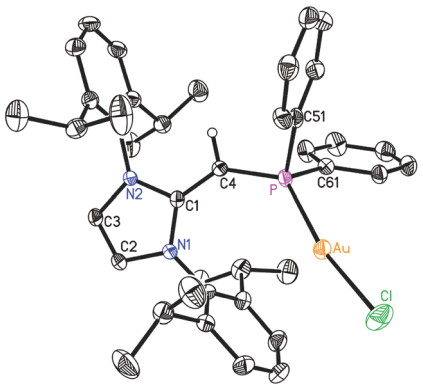

Fig. 8 Molecular structure of **9** with thermal ellipsoids at the 30% probability level. The hydrogen atom attached to C(4) is shown with an arbitrarily small thermal parameter; all other hydrogens have been omitted for clarity. Selected bond lengths (Å) and angles (°): Au–P 2.2334(8), Au–Cl 2.2914(10), P–C(4) 1.741(3), C(1)–C(4) 1.381(4), P–C(51) 1.831(3), P–C(61) 1.826(3); P–Au–Cl 168.72(4), C(4)–P–Au 128.48(11), P–C(4)–C(1) 136.9(3), C(4)–P–C(51) 99.84(15), C(4)–P–C(61) 109.43(15), Au–P–C(51) 106.45(11), Au–P–C(61) 106.46(11).

In an attempt to prepare a more reactive Au(I) complex for future catalytic trials,[20d] the NHO–Au complex (IPr=CH)-Ph$_2$P·AuCl **9** was treated with Na[BAr$^F{}_4$] ([BAr$^F{}_4$]$^-$ = (3,5-(F$_3$C)$_2$C$_6$H$_3$)$_4$B) in toluene. This reaction afforded a gummy orange precipitate from which a product of [BAr$^F{}_4$]$^-$ anion activation [IPr-CH$_2$-PPh$_2$·Au(3,5-(F$_3$C)$_2$C$_6$H$_3$)]BAr$^F{}_4$ **10** could be isolated and structurally characterized (eqn (5); Fig. 9). While the mechanism of this process is under investigation, protonation of the exocyclic olefin within the NHO unit occurred to yield an imidazolium-alkylphosphine ligand,[8] along with the removal of one Ar^F unit from the generally unreactive weakly coordinating [BAr$^F{}_4$]$^-$ anion. One possible source of the proton would be C–H activation of the backbone olefin within the IPr unit.[22] The generation of a highly electron deficient Au(I) center during the reaction process could facilitate the abstraction of Ar^F from the [BAr$^F{}_4$]$^-$ anion; although rare, related pro-

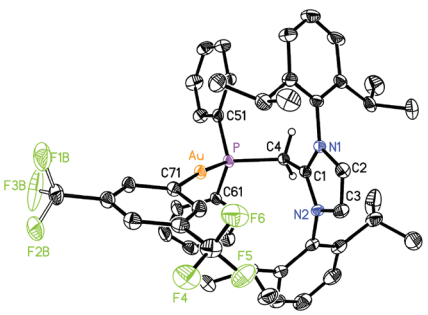

Fig. 9 Molecular structure of **10** with thermal ellipsoids at the 30% probability level. The hydrogen atoms attached to C(4) is shown with an arbitrarily small thermal parameter; all other hydrogen atoms and the B(3,5-(F$_3$C)$_2$C$_6$H$_3$)$_4^-$ anion have been omitted for clarity. Selected bond lengths (Å) and angles (°): Au–P 2.2798(8), Au–C(71) 2.070(23), P–C(4) 1.864(4), C(1)–C(4) 1.487(4); P–Au–C(71) 174.82(11), C(4)–P–Au 112.43(11), C(1)–C(4)–P 116.5(2).

cesses have been noted with both phosphine and NHC-bound Au(I) centers.[23] The structure of **10** is shown in Fig. 9 and, as expected, a nearly linear coordination geometry exists at the Au(I) center [P–Au–C(71) angle = 174.82(11)°]. The coordinative Au–P interaction in **10** [2.2798(8) Å] is only marginally elongated in relation to the Au–P distance in (IPr=CH)^{i}Pr$_2$P·AuCl **8** [2.2348(5) Å], while the adjacent P–C(4) bond length in **10** is longer by *ca.* 0.12 Å when compared to the P–C(4) distance in **8** as a result of a hybridization change at carbon from sp^2 in **8** to sp^3 in **10**. No reaction was observed when (IPr=CH)Ph$_2$P·AuCl **9** was treated with Na[SbF$_6$].

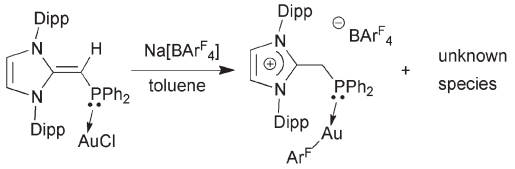

9 **10**

Ar^F = (3,5-(F$_3$C)$_2$C$_6$H$_3$) (5)

To further evaluate the donation abilities of the new phosphines, we targeted the preparation of NHOP·Rh(CO)$_2$Cl complexes with the hope of obtaining informative ν(CO) IR data.[3d] When the NHOPs **2** and **3** were each combined with 0.5 equiv. of [RhCl(CO)$_2$]$_2$, three different Rh–P containing products were found, as evidenced by ^{31}P{^{1}H} NMR spectroscopy in the form of doublet resonances due to coupling to Rh (I = 1/2). Despite multiple attempts, we could not separate the products due to their similar solubilities in common organic solvents, and as such further investigations were not pursued.

Divergent coordination chemistry of (IPr=CH)NMe$_2$ 4

As presented above, the NHOPs **2** and **3** exclusively bind to Lewis acidic units through the terminal phosphine residues. However in the corresponding amine-capped NHOs (such as **4**) featuring hard N-donor sites, there exists a chance that olefin coordination could transpire with soft Lewis acids (Chart 1). Somewhat to our surprise, (IPr=CH)NMe$_2$ **4** did not yield clean reactivity with THF·BH$_3$, with multiple products identified by ^{11}B NMR spectroscopy. In contrast, an isolable 1 : 1 complex (IPr=CH)NMe$_2$·AuCl **11** formed as a yellow solid in 89% yield when **4** was combined with Me$_2$S·AuCl in toluene (eqn (6)). The most drastic change in the ^{13}C{^{1}H} NMR spectra of the (IPr=CH)NMe$_2$ units was the upfield shift of the olefinic *C*HNMe$_2$ carbon from 89.0 ppm in free (IPr=CH)NMe$_2$ **4** to a position of 58.4 ppm in **11**; this latter spectroscopic signature suggested possible olefin coordination to gold in **11**. Crystals of **11** were obtained for X-ray crystallographic analysis and despite the lower quality of the data, (IPr=CH)NMe$_2$ coordination through a C–Au linkage was confirmed with a distance of 2.044(15) Å; moreover a nearly linear geometry was present at gold [C(3)–Au–Cl angle = 177.6(4)°; see Fig. S32 in the ESI†]. Therefore one can see direct evidence for the two possible binding modes of NHO-supported amines and phosphines in this study (Chart 2).

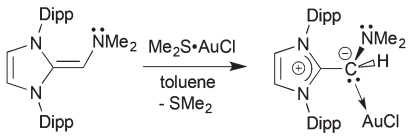

4 **11** (6)

Conclusion

We have reported efficient syntheses of neutral N-heterocyclic olefin-appended phosphines and amine donors, and present preliminary coordination behavior with the Lewis acids BH$_3$ and AuCl. Interestingly, modulation of the donor properties enables either NHO-based coordination (*via* an olefinic carbon atom) or standard phosphine binding modes to be adopted. As a result, we are exploring these coordinatively versatile ligands within the context of late metal-mediated catalysis.

Experimental

General

All reactions were performed in either an inert atmosphere glove box (Innovative Technology, Inc.) or using Schlenk techniques. Solvents were dried using a Grubbs-type solvent purification system[24] manufactured by Innovative Technologies, Inc. and stored under an atmosphere of nitrogen prior to use. Chlorodiisopropylphosphine, chlorodiphenylphosphine, *N*,*N*-dimethyliminium iodide ([Me$_2$N=CH$_2$]I), borane tetrahydrofuran complex, dimethylsulfide gold(I) chloride, Na[SbF$_6$], and [PdCl(cinnamyl)]$_2$ were used as received from Sigma Aldrich. Na[(3,5-(F$_3$C)$_2$C$_6$H$_3$)$_4$B] was obtained from Sigma Aldrich and dried under vacuum at 100 °C for 12 h prior to use. IPr=CH$_2$ **1** [3d] and IPr[25] were prepared according to literature procedures. ^{1}H, ^{1}H{^{31}P}, ^{13}C{^{1}H}, ^{31}P{^{1}H}, ^{11}B, and ^{11}B{^{1}H} NMR spectra were recorded on a Varian VNMRS-400 or Varian VNMRS-500 spectrometer and referenced externally to SiMe$_4$, 85% H$_3$PO$_4$, or F$_3$B·OEt$_2$. Elemental analyses were performed by the Analytical and Instrumentation Laboratory at the University of Alberta. Melting points were measured in sealed glass capillaries under nitrogen using a MelTemp melting point apparatus and are uncorrected.

X-ray crystallography

Crystals for X-ray diffraction studies were removed from a vial and immediately coated with thin a layer of hydrocarbon oil (Paratone-N). A suitable crystal was then mounted on a glass fiber, and quickly placed in a low temperature stream of nitrogen on the X-ray diffractometer. All data (Tables 1 and 2) were collected using a Bruker APEX II CCD detector/D8 diffractometer using Mo Kα or Cu Kα radiation with the crystals cooled to −80 °C or −100 °C. The data was corrected for absorption through Gaussian integration from the indexing of the crystal faces. Crystal structures were solved using intrinsic phasing SHELXT[26] (**2**, **4**, **5**, **6**, **9** and **11**), direct methods (**3**), or Patterson/structure expansion (**7** and **8**)[27] and refined using full-matrix

Table 1 Crystallographic data for compounds **2–6**

	(IPr=CH)P^{i}Pr$_2$ (**2**)	(IPr=CH)PPh$_2$ (**3**)	(IPr=CH)NMe$_2$ (**4**)	(IPr=CH)^{i}Pr$_2$P·BH$_3$ (**5**·0.5C$_6$H$_{14}$)	(IPr=CH)Ph$_2$P·BH$_3$ (**6**)
CCDC number	1448851	1448848	1448850	1448846	1448845
Formula	$C_{34}H_{51}N_2P$	$C_{40}H_{47}N_2P$	$C_{30}H_{43}N_3$	$C_{35.50}H_{57.50}BN_2P$	$C_{40}H_{50}BN_2P$
Formula weight	518.73	586.76	445.67	554.11	600.60
Cryst. dimens. (mm)	0.34 × 0.17 × 0.17	0.21 × 0.18 × 0.07	0.20 × 0.15 × 0.08	0.49 × 0.08 × 0.06	0.24 × 0.20 × 0.12
Crystal system	Monoclinic	Monoclinic	Monoclinic	Trigonal	Monoclinic
Space group	$P2_1/c$	$P2_1/c$	$P2_1/n$	$R\bar{3}$	$P2_1/n$
Unit cell dimensions					
a (Å)	21.3382(6)	10.7803(2)	9.3774(2)	42.1750(6)	10.7033(2)
b (Å)	18.3587(5)	16.7651(3)	20.2169(4)		18.7813(3)
c (Å)	17.2832(4)	39.0845(6)	20.2169(4)	10.4933(2)	17.9853(3)
β (°)	33.3817(9)	95.7606(9)	100.0916(11)		92.3243(8)
V (Å^3)	13053.4(6)	7028.2(2)	2799.90(10)	16164.1(6)	3612.46(11)
Z	16	8	4	18	4
ρ calcd (g cm^{-3})	1.056	1.109	1. 057	1.025	1.104
μ (mm^{-1})	0.897	0.894	0.463	0.835	0. 874
Temperature (°C)	−100	−100	−100	−100	−100
$2\theta_{max}$ (°)	146.35	146.98	148.31	148.11	145.02
Total data	75117	48 771	108 108	38 050	24 968
Unique data (R_{int})	25 575 (0.0449)	13 861 (0.0370)	5659 (0.0433)	7292 (0.0561)	7118 (0.0257)
Obs [$I > 2\sigma(I)$]	17 632	11 433	5104	6290	6558
R_1 [$F_o^2 \geq 2\sigma(F_o^2)$][a]	0.0698	0.0461	0.0417	0.0497	0.0371
wR_2 [all data]	0.2012	0.1292	0.1151	0.1428	0.1037
Max/min Δr (e Å^{-3})	0.954/−0.511	0. 444/−0.299	0.238/−0.256	0.552/−0.453	0.311/−0.366

[a] $R_1 = \sum||F_o| - |F_c||/\sum|F_o|$; $wR_2 = [\sum w(F_o^2 - F_c^2)^2/\sum w(F_o^4)]^{1/2}$.

Table 2 Crystallographic data for compounds **7–10**

	(IPr=CH)^{i}Pr$_2$P·PdCl(cinnamyl) (**7**)	(IPr=CH)^{i}Pr$_2$P·AuCl (**8**)	(IPr=CH)Ph$_2$P·AuCl (**9**·0.5C$_7$H$_8$)	[IPr-CH$_2$–PPh$_2$·AuAr^F]-BAr$^F_4$ (**10**)
CCDC number	1448843	1448847	1448849	1448844
Formula	$C_{50}H_{68}ClN_2PPd$	$C_{34}H_{51}AuClN_2P$	$C_{43.50}H_{51}AuClN_2P$	$C_{80}H_{63}AuBF_{30}N_2P$
Formula weight	869.88	751.15	865.25	1861.07
Cryst. dimens. (mm)	0.14 × 0.13 × 0.10	0.32 × 0.18 × 0.16	0.19 × 0.18 × 0.06	0.48 × 0.13 × 0.01
Crystal system	Triclinic	Monoclinic	Monoclinic	Monoclinic
Space group	$P\bar{1}$	$P2_1/n$	$P2_1/c$	$P2_1/n$
Unit cell				
a (Å)	10.3535(3)	10.4781(4)	9.7488(6)	14.0570(4)
b (Å)	12.5649(4)	16.3684(6)	20.0872(13)	25.1328(6)
c (Å)	18.9321(6)	20.9256(7)	20.8717(14)	22.7564(7)
α (°)	72.828(2)			
β (°)	100.0916(11)	101.6635(4)	98.4585(10)	102.1003(18)
γ (°)	89.231(2)			
V (Å^3)	2304.58(13)	3514.8(2)	4042.8(5)	7861.0(4)
Z	2	4	4	4
ρ calcd (g cm^{-3})	1.254	1.419	1.422	1.573
μ (mm^{-1})	4.357	4.330	3.776	4.750
Temperature (°C)	−100	−80	−80	−100
$2\theta_{max}$ (°)	147.88	56.66	55.22	148.42
Total data	87 008	32 818	36 511	55 754
Unique data (R_{int})	8901 (0.1174)	8717 (0.0238)	9373 (0.0430)	12 419(0.0808)
Obs [$I > 2\sigma(I)$]	7672	7584	7578	7672
R_1 [$F_o^2 \geq 2\sigma(F_o^2)$][a]	0.0566	0.0200	0.0316	0.0420
wR_2 [all data]	0.1547	0.0532	0.0855	0.1156
Max/min Δr (e Å^{-3})	1.436/−1.103	1.076/−0.505	1.671/−1.292	1.078/−2.636

[a] $R_1 = \sum||F_o| - |F_c||/\sum|F_o|$; $wR_2 = [\sum w(F_o^2 - F_c^2)^2/\sum w(F_o^4)]^{1/2}$.

least-squares on F^2. The assignment of hydrogen atoms positions were based on the sp^2 or sp^3 hybridization of their attached carbon atoms, and were given thermal parameters 20% greater than those of their parent atoms.

Special refinement conditions

(IPr=CH)P^{i}Pr$_2$·BH$_3$ 5. Attempts to refine peaks of residual electron density as disordered or partial-occupancy solvent hexane carbon atoms were unsuccessful. The data were cor-

rected for disordered electron density through use of the SQUEEZE procedure as implemented in PLATON.[28] A total solvent-accessible void volume of 1145 Å^3 with a total electron count of 212 (consistent with 4.24 molecules of solvent hexane, or ~0.25 molecules per formula unit of **5**) was found in the unit cell.

(IPr═CH)P^{i}Pr$_2$·PdCl(cinnamyl) 7. The crystal used for data collection was found to display non-merohedral twinning. Both components of the twin were indexed with the program CELL_NOW (Bruker AXS, Inc., Madison, WI, 2004). The second twin component can be related to the first component by a 7.4° rotation about the [0.2 1 −0.35] axis in real space and about the [0.1 1 −0.4] axis in reciprocal space. Integrated intensities for the reflections from the two components were written into a SHELXL-2014[26] HKLF 5 reflection file with the data integration program SAINT (version 8.34A), using all reflection data (exactly overlapped, partially overlapped and non-overlapped). The refined value of the twin fraction (SHELXL-2014 BASF parameter) was 0.3198(17).

(IPr═CH)PPh$_2$·AuCl 9. Attempts to refine peaks of residual electron density as disordered or partial-occupancy solvent toluene or hexane carbon atoms were unsuccessful. The data were corrected for disordered electron density through use of the SQUEEZE procedure as implemented in PLATON.[28] A total solvent-accessible void volume of 517 Å^3 with a total electron count of 110 (consistent with 2 molecules of solvent toluene, or 0.5 molecules per formula unit of the Au complex) was found in the unit cell.

Synthetic details

Synthesis of (IPr═CH)P^{i}Pr$_2$ 2. ^{i}Pr$_2$PCl (100 μL, 0.77 mmol) was added dropwise to IPr═CH$_2$ **1** (0.508 g, 1.26 mmol) in 8 mL of THF. The resulting mixture was stirred for 20 h to give an orange suspension. The mixture was then filtered and the volatiles were removed from the filtrate to afford an orange solid that was extracted with 4 mL of hexanes and filtered again. Removal of the volatiles from the filtrate gave **2** as a light brown solid (0.267 g, 81%). Crystals suitable for X-ray crystallography were obtained by cooling (−30 °C) a saturated solution of **2** in hexanes. ^{1}H NMR (400 MHz, C_6D_6): δ 7.26–7.11 (m, 6H, Ar*H*), 5.88 (dd, $^3J_{HH}$ = 2.4 Hz, $^5J_{HH}$ = 0.8 Hz, 1H, NC*H*CHN), 5.85 (dd, $^3J_{HH}$ = 2.4 Hz, $^5J_{HH}$ = 0.8 Hz, 1H, NC*H*CHN), 3.28 (overlapping septets, 4H, ArC*H*(CH$_3$)$_2$), 2.66 (d, $^2J_{HP}$ = 5.6 Hz, 1H, C*H*P^{i}Pr$_2$), 1.45 (d, $^3J_{HH}$ = 7.2 Hz, 6H, ArCH(C*H*$_3$)$_2$), 1.33 (d, $^3J_{HH}$ = 7.2 Hz, 6H, ArCH(C*H*$_3$)$_2$), 1.25 (broad septet, $^3J_{HH}$ = 7.2 Hz, 2H, PC*H*(CH$_3$)$_2$), 1.18 (d, $^3J_{HH}$ = 6.8 Hz, 6H, ArCH(C*H*$_3$)$_2$), 1.15 (d, $^3J_{HH}$ = 6.8 Hz, 6H, ArCH(C*H*$_3$)$_2$), 0.96 (dd, $^3J_{HH}$ = 7.2 Hz, $^3J_{HP}$ = 11.6 Hz, 6H, PCH(CH$_3$)C*H*$_3$), 0.90 (dd, $^3J_{HH}$ = 6.8 Hz, $^3J_{HP}$ = 12.8 Hz, 6H, PCH(CH$_3$)C*H*$_3$). ^{13}C{^{1}H} (126 MHz, C_6D_6): δ 154.5 (Ar–*C*), 154.3 (Ar–*C*), 148.7 (Ar–*C*), 148.1 (Ar–*C*), 134.6 (N*C*N), 129.7 (Ar–*C*), 129.4 (Ar–*C*), 124.6 (Ar–*C*), 123.9 (Ar–*C*), 117.8 (HC*C*H), 115.0 (HC*C*H), 51.4 (d, $^1J_{CP}$ = 114.7 Hz, H*C*P^{i}Pr$_2$), 29.1 (Ar*C*H(CH$_3$)$_2$), 28.7 (Ar*C*H(CH$_3$)$_2$), 26.5 (d, $^2J_{CP}$ = 11.1 Hz, PCH(*C*H$_3$)$_2$), 25.9 (ArCH(*C*H$_3$)$_2$), 24.9 (ArCH(*C*H$_3$)$_2$), 23.4 (ArCH(*C*H$_3$)$_2$), 22.6 (ArCH(*C*H$_3$)$_2$). ^{31}P{^{1}H} NMR (160 MHz, C_6D_6): δ −17.4. Mp (°C): 132–135. Anal. Calcd for $C_{34}H_{51}N_2P$: C, 78.72; H, 9.91; N, 5.40. Found: C, 77.76; H 9.85; N, 5.21.

Synthesis of (IPr═CH)PPh$_2$ 3. Ph$_2$PCl (41.2 μL, 0.16 mmol) was added dropwise to a solution of IPr═CH$_2$ **1** (0.150 g, 0.37 mmol) in 3 mL of THF. The resulting mixture was stirred overnight to give an orange suspension. The precipitate was allowed to settle and the mother liquor was isolated after filtration. The volatiles were removed from the mother liquor to afford (IPr═CH)PPh$_2$ **3** as a brown solid (0.078 g, 83%). Crystals suitable for X-ray crystallography were obtained by cooling (−30 °C) a saturated solution in hexanes. ^{1}H NMR (400 MHz, C_6D_6): δ 7.35–6.92 (m, 16H, Ar*H* and Ph*H*), 5.92 (s, 2H, N(C*H*)$_2$N), 3.34 (d, $^3J_{HP}$ = 5.6 Hz, 1H, C*H*PPh$_2$), 3.26 (overlapping septets, 4H, ArC*H*(CH$_3$)$_2$), 1.33 (d, $^3J_{HH}$ = 7.2 Hz, 6H, ArCH(C*H*$_3$)$_2$), 1.19 (d, $^3J_{HH}$ = 7.0 Hz, 6H, ArCH(C*H*$_3$)$_2$), 1.18 (d, $^3J_{HH}$ = 7.0 Hz, 6H, ArCH(C*H*$_3$)$_2$), 1.12 (d, $^3J_{HH}$ = 7.2 Hz, 6H, ArCH(C*H*$_3$)$_2$). ^{13}C{^{1}H} NMR (126 MHz, C_6D_6): δ 154.0 (d, $^1J_{CP}$ = 35 Hz, Ph–*C*), 148.5 (Ar–*C*), 147.9 (Ar–*C*), 146.2 (d, $^2J_{CP}$ = 13 Hz, Ph–*C*), 136.6 (Ar–*C*), 134.2 (Ar–*C*), 132.3 (d, $^2J_{CP}$ = 20 Hz, Ph–*C*), 130.0 (Ar–*C*), 129.7 (Ar–*C*), 127.7 (Ar–*C*), 126.8 (Ar–*C*), 124.5 (d, $^1J_{CP}$ = 41 Hz, Ph–*C*), 117.1 (HC*C*H), 115.5 (HC*C*H), 52.7 (H*C*PPh$_2$), 29.1 (*C*H(CH$_3$)$_2$), 28.8 (*C*H(CH$_3$)$_2$), 25.1 (CH(*C*H$_3$)$_2$), 24.7 (CH(*C*H$_3$)$_2$), 23.4 (CH(*C*H$_3$)$_2$), 22.5 (CH(*C*H$_3$)$_2$). ^{31}P{^{1}H} NMR (162 MHz, C_6D_6): δ −31.4. Mp (°C): 172–176. Anal. Calcd for $C_{40}H_{47}N_2P$: C, 81.87; H, 8.07; N, 4.77. Found: C, 81.34; H 8.33; N, 5.05.

Synthesis of IPr═CHNMe$_2$ 4. A solution of IPr (0.481 g, 1.24 mmol) in 3 mL of toluene was added to finely ground [H$_2$C═N(CH$_3$)$_2$]I (0.115 g, 0.62 mmol). The resulting mixture was stirred overnight to give a cloudy yellow reaction mixture. The mother liquor was isolated after filtration. The volatiles were then removed from the mother liquor to afford a yellow solid that was extracted with 2 mL of hexanes and filtered. Removal of the volatiles from the filtrate afforded **4** as a yellow solid (227 mg, 82%, product also contained 7% of unreacted IPr). Further purification can be performed by adding BPh$_3$ (*ca.* 2 mg) to **4** (0.050 g) in minimal amount of benzene (*ca.* 0.5 mL). The solution was stirred for 15 min and 2 mL of hexanes was added to yield a white precipitate. The mother liquor was isolated after filtration and the volatiles were removed from the filtrate to afford **4** (0.040 g) containing <1% of unreacted IPr. Crystals suitable for X-ray crystallography were obtained by cooling (−30 °C) a saturated solution in hexanes. ^{1}H NMR (500 MHz, C_6D_6): δ 7.23 (t, $^3J_{HH}$ = 7.5 Hz, 2H, Ar*H*), 7.14 (d, $^3J_{HH}$ = 8.0 Hz, 4H, Ar*H*), 5.86 (dd, $^3J_{HH}$ = 2.5 Hz, $^5J_{HH}$ = 1.0 Hz, 1H, *H*CCH), 5.77 (d, $^3J_{HH}$ = 2.0 Hz, 1H, HCC*H*), 3.51 (septet, $^3J_{HH}$ = 7.0 Hz, 2H, C*H*(CH$_3$)$_2$), 3.47 (s, 1H, C*H*N(CH$_3$)$_2$), 3.36 (septet, $^3J_{HH}$ = 7.0 Hz, 2H, C*H*(CH$_3$)$_2$), 1.97 (s, 6H, N(C*H*$_3$)$_2$), 1.41 (d, $^3J_{HH}$ = 7.0 Hz, 6H, CH(C*H*$_3$)$_2$), 1.38 (d, $^3J_{HH}$ = 7.0 Hz, 6H, CH(C*H*$_3$)$_2$), 1.27 (d, $^3J_{HH}$ = 7.0 Hz, 6H, CH(C*H*$_3$)$_2$), 1.22 (d, $^3J_{HH}$ = 7.0 Hz, 6H, CH(C*H*$_3$)$_2$). ^{13}C{^{1}H} NMR (126 MHz, C_6D_6): δ 149.0 (Ar–*C*), 148.1 (Ar–*C*), 145.0 (Ar–*C*), 138.1 (N*C*N), 129.1 (Ar–*C*), 128.3 (Ar–*C*), 124.6 (Ar–*C*), 123.1 (Ar–*C*), 117.4 (HC*C*H), 114.4 (HC*C*H), 89.0 (HC*N*(CH$_3$)$_2$), 49.8 (*C*H(CH$_3$)$_2$), 28.7 (N(*C*H$_3$)$_2$), 28.6 (N(*C*H$_3$)$_2$), 25.6 (CH(*C*H$_3$)$_2$), 24.4 (CH(*C*H$_3$)$_2$), 23.8 (CH(*C*H$_3$)$_2$), 22.9 (CH(*C*H$_3$)$_2$). Mp (°C): 89–94. Anal. Calcd for $C_{30}H_{43}N_3$: C, 80.85; H, 9.72; N, 9.43.

Found: C, 79.04; H 9.43; N, 8.52. Despite repeated attempts, analyses were consistently low in the carbon content. See Fig. 7 and 8 in the ESI† for a copy of the NMR spectra of **4**.

Preparation of (IPr═CH)P^{i}Pr$_2$·BH$_3$ 5. 106 μL of THF·BH$_3$ (1.0 M solution in THF, 0.11 mmol) was added dropwise to a solution of IPr═CHP^{i}Pr$_2$ **2** (50 mg, 0.096 mmol) in 2 mL of hexanes. The reaction mixture was stirred for 1.5 h and then filtered. The volatiles were removed from the filtrate and the resulting solid was dissolved in approximately 0.5 mL of hexanes and cooled (−30 °C) to afford (IPr═CH)P^{i}Pr$_2$·BH$_3$ as a white microcrystalline solid (27 mg, 52%). Crystals suitable for X-ray crystallography were obtained by cooling (−30 °C) a saturated solution in hexanes. ^{1}H NMR (500 MHz, C$_6$D$_6$): δ 7.24 (t, $^3J_{HH}$ = 7.5 Hz, 2H, Ar*H*), 7.17 (d, $^3J_{HH}$ = 8.0 Hz, 4H, Ar*H*), 5.87 (s, 2H, N(C*H*)$_2$N), 3.16 (septet, $^3J_{HH}$ = 7.0 Hz, 4H, ArC*H*(CH$_3$)$_2$), 2.09 (d, $^2J_{HP}$ = 10.0 Hz, 1H, C*H*P^{i}Pr$_2$), 1.44 (d, $^3J_{HH}$ = 6.5 Hz, 12H, C*H*(CH$_3$)$_2$), 1.44 (broad septet, 2H, P(C*H*(CH$_3$)$_2$)$_2$), 1.14 (d, $^3J_{HH}$ = 6.5 Hz, 12H, ArCH(C*H*$_3$)$_2$), 1.06 (dd, $^3J_{HH}$ = 7.0 Hz, $^3J_{HP}$ = 14.5 Hz, 6H, PCH(C*H*$_3$)$_2$), 0.93 (dd, $^3J_{HH}$ = 7.0 Hz, $^3J_{HP}$ = 13.5 Hz, 6H, PCH(C*H*$_3$)$_2$), 0.25 (broad d, $^2J_{HP}$ = 15.0 Hz, 3H, B*H*$_3$). ^{13}C{^{1}H} NMR (126 MHz, C$_6$D$_6$): δ 154.3 (d, $^2J_{CP}$ = 11.6 Hz, N*C*N), 147.9 (Ar–*C*), 130.2 (Ar–*C*), 128.4 (Ar–*C*), 128.2 (Ar–*C*), 128.0 (Ar–*C*), 124.8 (N(*C*H)$_2$N), 40.2 (d, $^1J_{CP}$ = 73.8 Hz, H*C*P^{i}Pr$_2$), 28.8 (Ar*C*H(CH$_3$)$_2$), 26.7 (d, $^2J_{CP}$ = 39.5 Hz, P(CH(*C*H$_3$)$_2$)$_2$), 25.3 (ArCH(*C*H$_3$)$_2$), 22.9 (ArCH(*C*H$_3$)$_2$), 17.2 (d, $^1J_{CP}$ = 58.9 Hz, P(*C*H(CH$_3$)$_2$)$_2$). ^{11}B{^{1}H} NMR (160 MHz, C$_6$D$_6$): δ −42.0. ^{31}P{^{1}H} NMR (201 MHz, C$_6$D$_6$): δ 21.9. Mp (°C): 154–156. Anal. Calcd for C$_{34}$H$_{54}$BN$_2$P: C, 76.67; H, 10.22; N, 5.26. Found: C, 75.94; H 10.10; N, 5.42.

Preparation of (IPr═CH)PPh$_2$·BH$_3$ 6. 93.8 μL of THF·BH$_3$ (1.0 M solution in THF, 0.094 mmol) was added dropwise to a solution of IPr═CHPPh$_2$ **3** (50.0 mg, 0.085 mmol) in 2 mL of hexanes. The reaction mixture was stirred for 90 min. The solvent volume was reduced *in vacuo* until the mixture just turned cloudy and then cooled (−30 °C) to afford **6** as an off-white microcrystalline solid (29 mg, 56%). Crystals suitable for X-ray crystallography were obtained by slow evaporation of a saturated solution of (IPr═CH)PPh$_2$·BH$_3$ **6** in toluene at room temperature. ^{1}H NMR (500 MHz, C$_6$D$_6$): δ 7.69–7.71 (m, 4H, Ph*H*), 7.72 (t, $^3J_{HH}$ = 7.5 Hz, 2H, Ar*H*), 7.12 (d, $^3J_{HH}$ = 8.0 Hz, 4H, Ar*H*), 6.98–6.95 (m, 6H, Ph*H*), 5.93 (s, 2H, N(C*H*)$_2$N), 3.15 (septet, $^3J_{HH}$ = 7.0 Hz, 4H, C*H*(CH$_3$)$_2$), 2.83 (d, $^2J_{HP}$ = 9.5 Hz, 1H, C*H*PPh$_2$), 1.24 (d, $^3J_{HH}$ = 7.0 Hz, 12H, CH(C*H*$_3$)$_2$), 1.12 (d, $^3J_{HH}$ = 7.0 Hz, 12H, CH(C*H*$_3$)$_2$), 0.98 (broad d, $^2J_{HP}$ = 16.0 Hz, 3H, B*H*$_3$). ^{13}C{^{1}H} NMR (126 MHz, C$_6$D$_6$): δ 153.2 (d, $^2J_{CP}$ = 15.6 Hz, N*C*N), 147.7 (Ar–*C*), 137.7 (d, $^1J_{CP}$ = 58.7 Hz, Ph–*C*), 132.0 (d, J_{CP} = 9.3 Hz, Ph–*C*), 130.4 (Ar*C*), 129.1 (d, J_{CP} = 2.0 Hz, Ph–*C*), 128.3 (Ar–*C*), 128.0 (d, J_{CP} = 9.5 Hz, Ph–*C*), 125.0 (N(*C*H)$_2$N), 117.6 (Ar–*C*), 44.2 (d, $^1J_{CP}$ = 84.8 Hz, H*C*PPh$_2$), 29.0 (*C*H(CH$_3$)$_2$), 25.2 (CH(*C*H$_3$)$_2$), 22.8 (CH(*C*H$_3$)$_2$). ^{11}B{^{1}H} NMR (128 MHz, C$_6$D$_6$): δ −35.8. ^{31}P{^{1}H} NMR (162 MHz, C$_6$D$_6$): δ 7.3. Mp (°C): 164–170. Anal. Calcd for C$_{40}$H$_{50}$BN$_2$P: C, 79.99; H, 8.39; N, 4.66. Found: C, 79.36; H 8.38; N, 4.68.

Reaction of IPr═CHNMe$_2$ with THF·BH$_3$. 63.8 μL of THF·BH$_3$ (1.0 M solution in THF, 0.058 mmol) was added dropwise to a solution of IPr═CHNMe$_2$ **4** (26 mg, 0.058 mmol) in 1 mL of hexanes. Once THF·BH$_3$ was added the yellow solution became colorless. The reaction was stirred for approximately 2 hours and then the volatiles were removed. ^{11}B NMR analysis showed that there was no THF·BH$_3$ remaining, however 5 new unidentifiable products were formed; attempts to obtain pure products were not successful.

Reaction of (IPr═CH)P^{i}Pr$_2$ with [PdCl(cinnamyl)]$_2$. [PdCl(cinnamyl)]$_2$ (0.024 g, 0.046 mmol) was combined with (IPr═CH)P^{i}Pr$_2$ **2** (0.048 g, 0.093 mmol) in 2 mL of toluene. The reaction mixture rapidly became yellow in color. The solution was left to stir overnight to yield a red solution and the volatiles were removed. ^{1}H and ^{31}P NMR spectroscopy showed a mixture of several products. On one occasion, yellow crystals (2–3 mg) suitable for X-ray crystallography were obtained by cooling (−30 °C) a saturated solution of the reaction mixture in toluene/hexanes. Data for (IPr═CH)P^{i}Pr$_2$·PdCl(cinnamyl) **7**. ^{1}H NMR (400 MHz, C$_6$D$_6$): δ 7.55 (d, $^3J_{HH}$ = 8.0 Hz, 2H, Ar*H*), 7.22–7.00 (m, 8H, Ph*H* and Ar*H*), 5.90 (s, 2H, N(C*H*)$_2$N), 5.41 (ddd, J_{HH} = 13.2 Hz, J_{HH} = 9.2 Hz, J_{HH} = 9.2 Hz, 1H, CH$_2$C*H*CHPh), 4.98 (m, 3H, C*H*$_2$CHC*H*Ph), 4.01 (broad d, $^3J_{HP}$ = 11.2 Hz, 3H, PCH(C*H*$_3$)$_2$), 3.49 (broad d, $^3J_{HP}$ = 6.8 Hz, 3H, PCH(C*H*$_3$)$_2$), 3.23 (broad septet, 4H, ArC*H*(CH$_3$)$_2$), 2.79 (broad s, (IPr═C*H*)P^{i}Pr$_2$), 2.44 (broad d, $^3J_{HH}$ = 12.0 Hz, 3H, PCH(C*H*$_3$)$_2$), 1.88 (broad s, 3H, PCH(C*H*$_3$)$_2$), 1.38 (broad m, 12H, ArCH(C*H*$_3$)$_2$), 1.14 (broad m, 1H, PC*H*(CH$_3$)$_2$), 1.06 (d, $^3J_{HH}$ = 6.8 Hz, 12H, ArCH(C*H*$_3$)$_2$). ^{31}P{^{1}H} NMR (162 MHz, C$_6$D$_6$): δ 34.0. We did not have enough sample to record a meaningful ^{13}C{^{1}H} NMR spectrum.

Synthesis of (IPr═CH)P^{i}Pr$_2$·AuCl 8. A solution of (IPr═CH)P^{i}Pr$_2$ **2** (99 mg, 0.19 mmol) in 5 mL of toluene was added dropwise to solid Me$_2$S·AuCl (56 mg, 0.19 mmol) to give a yellow solution. This reaction mixture was stirred at room temperature for 2 hours and a small amount of metallic precipitate was observed. The mixture was then filtered and the volatiles were then removed from the filtrate to afford (IPr═CH)P^{i}Pr$_2$·AuCl **8** as a pale yellow solid (121 mg, 85%). Crystals suitable for X-ray crystallography were obtained by cooling (−30 °C) a saturated solution in a 1 : 1 mixture of toluene/hexanes. ^{1}H NMR (500 MHz, C$_6$D$_6$): δ 7.49 (t, $^3J_{HH}$ = 7.0 Hz, 2H, Ar*H*), 7.23 (d, $^3J_{HH}$ = 8.0 Hz, 4H, Ar*H*), 5.78 (s, 2H, N(C*H*)$_2$N), 3.01 (septet, $^3J_{HH}$ = 7.0 Hz, 4H, ArC*H*(CH$_3$)$_2$), 2.22 (d, $^2J_{HP}$ = 6.0 Hz, 1H, C*H*P^{i}Pr$_2$), 1.38 (d, $^3J_{HH}$ = 7.0 Hz, 12H, ArC*H*(CH$_3$)$_2$), 1.28 (septet, $^3J_{HH}$ = 8.0 Hz, 2H, P(C*H*(CH$_3$)$_2$)$_2$), 1.07 (d, $^3J_{HH}$ = 7.0 Hz, 12H, ArCH(C*H*$_3$)$_2$), 0.87 (dd, $^3J_{HH}$ = 7.0 Hz, $^3J_{HP}$ = 18.0 Hz, 6H, PCH(C*H*$_3$)$_2$), 0.80 (dd, $^3J_{HH}$ = 7.0 Hz, $^3J_{HP}$ = 16.0 Hz, 6H, PCH(C*H*$_3$)$_2$). ^{13}C{^{1}H} NMR (126 MHz, C$_6$D$_6$): δ 153.7 (d, $^2J_{CP}$ = 10.3 Hz, N*C*N), 147.0 (Ar–*C*), 134.3 (Ar–*C*), 131.2 (Ar–*C*), 129.3 (Ar–*C*), 125.4 (Ar–*C*), 117.5 (N(*C*H)$_2$N), 40.7 (d, $^1J_{CP}$ = 81.3 Hz, H*C*P^{i}Pr$_2$), 29.3 (d, $^2J_{CP}$ = 41.6 Hz, P(CH(*C*H$_3$)$_2$)$_2$), 28.8 (Ar*C*H(CH$_3$)$_2$), 25.0 (ArCH(*C*H$_3$)$_2$), 23.2 (ArCH(*C*H$_3$)$_2$), 19.1 (d, $^1J_{CP}$ = 3.8 Hz, P(*C*H(CH$_3$)$_2$)$_2$), 18.3 (ArCH(*C*H$_3$)$_2$). ^{31}P{^{1}H} NMR (201 MHz, C$_6$D$_6$): δ 28.7. Mp (°C): 90 (decomp., turned black). Anal. Calcd for C$_{34}$H$_{51}$AuClN$_2$P: C, 54.36; H, 6.84; N, 3.73. Found: C, 54.82; H 6.86; N, 3.61.

Synthesis of (IPr═CH)PPh$_2$·AuCl 9. A solution of (IPr═CH)PPh$_2$ **3** (78 mg, 0.13 mmol) in 5 mL of toluene was slowly

added to solid Me_2S·AuCl (40 mg, 0.14 mmol) to give a yellow solution. This reaction mixture was stirred at room temperature for 90 minutes and a small amount of metallic precipitate was observed. The mixture was filtered and the volatiles were then removed from the filtrate to afford (IPr=CH)PPh_2·AuCl **9** as a pale yellow solid (108 mg, 98%). Crystals suitable for X-ray crystallography were obtained by cooling (−30 °C) a saturated solution in a 2 : 1 mixture of toluene/hexanes. ^{1}H NMR (400 MHz, C_6D_6): δ 7.47–7.49 (m, 4H, Ph*H*), 7.41 (t, $^3J_{HH}$ = 8.0 Hz, 2H, Ar*H*), 7.18 (d, $^3J_{HH}$ = 8.0 Hz, 4H, Ar*H*), 6.86–6.87 (m, 6H, Ph*H*), 5.83 (s, 2H, N(C*H*)$_2$N), 3.00 (septet, $^3J_{HH}$ = 6.8 Hz, 4H, C*H*(CH$_3$)$_2$), 2.80 (d, $^2J_{HP}$ = 6.4 Hz, 1H, C*H*PPh$_2$), 1.20 (d, $^3J_{HH}$ = 6.8 Hz, 12H, CH(C*H*$_3$)$_2$), 1.08 (d, $^3J_{HH}$ = 6.8 Hz, 12H, CH(C*H*$_3$)$_2$). ^{13}C{^{1}H} NMR (126 MHz, C_6D_6): δ 152.3 (d, $^2J_{CP}$ = 13.6 Hz, N*C*N), 146.9 (Ar–*C*), 139.1 (d, $^1J_{CP}$ = 63.9 Hz, Ph–*C*), 137.8 (Ar–*C*), 133.7 (Ar–*C*), 132.6 (d, $^2J_{CP}$ = 14.1 Hz, Ph–*C*), 131.4 (N(*C*H)$_2$N), 129.7 (d, J_{CP} = 2.3 Hz, Ph–*C*), 117.5 (Ar–*C*), 44.6 (d, $^1J_{CP}$ = 92.6 Hz, H*C*PPh$_2$), 29.0 (*C*H(CH$_3$)$_2$), 24.6 (CH(*C*H$_3$)$_2$), 23.1 (CH(*C*H$_3$)$_2$). ^{31}P{^{1}H} NMR (162 MHz, C_6D_6): δ 8.1. Mp (°C): 122 (decomp., turned black). Anal. Calcd for $C_{40}H_{47}AuN_2P$: C, 58.65; H, 5.78; N, 3.42. Found: C, 58.83; H 5.89; N, 3.13.

Reaction of IPr=CHPPh$_2$·AuCl and Na[BAr$^F_4$]: isolation of [IPr–CH$_2$–PPh$_2$·Au(3,5-(F$_3$C)$_2$C$_6$H$_3$)]BAr$^F_4$ 10. (IPr=CH)-PPh_2·AuCl **9** (17 mg, 0.020 mmol) and Na[BAr$^F_4$] (18 mg, 0.020 mmol) were combined in 2 mL of toluene and stirred at room temperature overnight. A pale orange solution formed along with a gummy orange precipitate. The mother liquor was decanted away and the precipitate was exposed to prolonged vacuum to yield an orange solid. This solid was then extracted with CH_2Cl_2 (2 × 1 mL) and the combined extracts were filtered. The filtrate was then layered with 2 mL of hexanes before cooling to −30 °C, leading to colorless crystals of **10** (19 mg). ^{1}H NMR (500 MHz, $CDCl_3$): δ 7.42 (broad d, $^3J_{HH}$ = 5.5 Hz, 2H, Ar^F–*H*), 7.69 (broad s, 8H, Ar*H* in BAr$^F_4$), 7.66 (s, 2H, N(C*H*)$_2$N), 7.64 (broad s, 1H, Ar^F–*H*), 7.52 (m, 6H, Ph–*H*), 7.40 (t, $^3J_{HH}$ = 7.5 Hz, 2H, Ar*H*), 7.29 (d, $^3J_{HH}$ = 8.0 Hz, 4H, Ar*H*), 7.23–7.25 (m, 4H, Ph–*H*), 6.94–6.98 (m, 4H, Ar*H* in BAr$^F_4$), 3.82 (d, $^2J_{HP}$ = 10.4 Hz, 2H, C*H*$_2$PPh$_2$), 2.82 (br, 4H, C*H*(CH$_3$)$_2$), 1.18 (d, $^3J_{HH}$ = 6.8 Hz, 12H, CH(C*H*$_3$)$_2$), 1.13 (d, $^3J_{HH}$ = 6.8 Hz, 12H, (CH(C*H*$_3$)$_2$). ^{11}B{^{1}H} NMR (128 MHz, $CDCl_3$): δ −6.6. ^{19}F NMR (376 MHz, $CDCl_3$): δ −62.3 [BAr$^F_4$$^-$], −62.6 [Au–Ar^F]. ^{31}P{^{1}H} NMR (162 MHz, $CDCl_3$): δ 34.4. ^{13}C{^{1}H} NMR (126 MHz, $CDCl_3$): δ 161.7 (q, $^1J_{CB}$ = 49.6 Hz, Ar–*C* in BAr$^F_4$$^-$), 146.7 (Ar–*C*), 144.9 (Ar–*C*), 137.9 (Ar–*C* in Au–Ar^F), 134.8 (Ar–*C* in BAr$^F_4$$^-$), 133.7 (Ar–*C*), 132.8 (Ar–*C*), 131.9 (d, J_{CP} = 14.0 Hz, Ar–*C*, 129.9 (d, J_{CP} = 19.5 Hz, Ar–*C*), 128.8 (q, $^1J_{CB}$ = 49.6 Hz in BAr$^F_4$$^-$), 126.2 (Ar–*C*), 125.6 (d, $^2J_{CP}$ = 12.7 Hz, Ar–*C*), 123.5 (Ar–*C*), 121.3 (N(*C*H)$_2$N), 119.9 (Ar–*C*), 117.5 (Ar–*C* in BAr$^F_4$$^-$), 30.0 (*C*H(CH$_3$)$_2$), 26.9 (H*C*PPh$_2$), 26.1 (CH(*C*H$_3$)$_2$), 22.7 (CH(*C*H$_3$)$_2$). The CF_3 groups in the Au–Ar^F unit could not be located in the ^{13}C{^{1}H} NMR spectrum. Mp (°C): 97 (decomp.; turned brown). Anal. Calcd for $C_{80}H_{63}AuBF_{30}N_2P$: C, 51.63; H, 3.41; N, 1.51. Found: C, 51.31; H, 3.62; N, 1.52.

Synthesis of (IPr=CH)NMe$_2$·AuCl 11. A solution of IPr=CHNMe$_2$ **4** (98 mg, 0.22 mmol) in 5 mL of toluene was added dropwise to solid Me_2S·AuCl (65 mg, 0.22 mmol) to give a dark yellow reaction mixture. This reaction mixture was stirred at room temperature for 90 minutes and a metallic precipitate was observed. The reaction mixture was then filtered and the volatiles were then removed from the filtrate to afford (IPr=CH)NMe_2·AuCl as a pale yellow solid (133 mg, 89%). Crystals of **11** were obtained by cooling a 2 : 1 toluene/hexanes solution overnight to −30 °C, however the low quality of the data prevents a detailed discussion of the metrical parameters (see Fig. S32 in the ESI†). ^{1}H NMR (400 MHz, C_6D_6): δ 7.13 (d, $^3J_{HH}$ = 9.0 Hz, 2H, Ar*H*), 7.01–7.04 (m, 4H, Ar*H*), 6.10 (s, 2H, N(C*H*)$_2$N), 4.02 (s, 1H, C*H*NMe$_2$), 3.04 (septet, $^3J_{HH}$ = 6.4 Hz, 4H, C*H*(CH$_3$)$_2$), 1.79 (broad s, 6 H, N(C*H*$_3$)$_2$), 1.47 (d, $^3J_{HH}$ = 6.4 Hz, 6H, CH(C*H*$_3$)$_2$), 1.47 (d, $^3J_{HH}$ = 6.4 Hz, 6H, CH(C*H*$_3$)$_2$), 0.95 (d, $^3J_{HH}$ = 7.2 Hz, 6H, CH(C*H*$_3$)$_2$), 0.95 (d, $^3J_{HH}$ = 7.2 Hz, 6H, CH(C*H*$_3$)$_2$). ^{13}C{^{1}H} NMR (126 MHz, C_6D_6): δ 161.0 (N*C*N), 147.5 (Ar–*C*), 145.3 (Ar–*C*), 132.2 (Ar–*C*), 131.2 (Ar–*C*), 124.7 (Ar–*C*), 124.5 (Ar–*C*), 120.8 (H*CC*H), 58.4 (H*C*N(CH$_3$)$_2$) 29.8 (CH(*C*H$_3$)$_2$), 29.4 (CH(*C*H$_3$)$_2$), 26.0 (CH(*C*H$_3$)$_2$), 25.9 (CH(*C*H$_3$)$_2$), 23.2 (N(*C*H$_3$)$_2$), 23.1 (N(*C*H$_3$)$_2$). Mp (°C): 123 (decomp., turned dark brown). Anal. Calcd $C_{30}H_{43}AuN_3$: C, 53.14; H, 6.39; N, 6.20. Found: C, 52.68; H, 6.33; N, 6.00.

Acknowledgements

This work was supported by the Natural Sciences and Engineering Research Council of Canada (Discovery Grant to E. R.; postgraduate scholarship to M. W. L.), Alberta Innovates-Technology Futures (New Faculty Award to E. R.), the Donors of the American Chemical Society Petroleum Research Fund, and The Killam Trust (postgraduate fellowship to M. W. L.).

Notes and references

1 (*a*) M. N. Hopkinson, C. Richter, M. Schedler and F. Glorius, *Nature*, 2014, **510**, 485; (*b*) M. C. Jahnke and F. E. Hahn, *Coord. Chem. Rev.*, 2015, **293**, 95; (*c*) D. J. Nelson and S. P. Nolan, *Chem. Soc. Rev.*, 2013, **42**, 6723; (*d*) A. Suzuki, *Angew. Chem., Int. Ed.*, 2011, **50**, 6722; (*e*) R. Martin and S. L. Buchwald, *Acc. Chem. Res.*, 2008, **41**, 1461; (*f*) C. M. Crudden and D. P. Allen, *Coord. Chem. Rev.*, 2004, **248**, 2247; (*g*) D. Bourissou, O. Guerret, F. P. Gabbaï and G. Bertrand, *Chem. Rev.*, 2000, **100**, 39; (*h*) For a review on cyclic(alkyl)aminocarbenes, see: M. Soleilhavoup and G. Bertrand, *Acc. Chem. Res.*, 2015, **48**, 256.

2 For selected review articles in this area, see: (*a*) L. J. Murphy, K. N. Robertson, J. D. Masuda and J. A. C. Clyburne, in *N-Heterocyclic Carbenes*, ed. S. P. Nolan, Wiley-VCH, Weinheim, 2014, pp. 427–497; (*b*) Y. Wang and G. H. Robinson, *Inorg. Chem.*, 2014, **53**, 11815; (*c*) E. Rivard, *Dalton Trans.*, 2014, **43**, 8577; (*d*) G. Prabusankar, A. Sathyanarayana, P. Suresh, C. N. Babu, K. Srinivas and B. P. R. Metla, *Coord. Chem. Rev.*, 2014, **269**, 96; (*e*) N. Kuhn and A. Al-Sheikh, *Coord. Chem. Rev.*, 2005, **249**, 829; (*f*) N. Burford and

P. J. Ragogna, *J. Chem. Soc., Dalton Trans.*, 2002, 4307; (*g*) C. Jones, *Chem. Commun.*, 2001, 2293.

3 (*a*) N. Kuhn, H. Bohnen, J. Kreutzberg, D. Bläser and R. Boese, *J. Chem. Soc., Chem. Commun.*, 1993, 1136; (*b*) C. E. I. Knappke, J. M. Neudörfl and A. J. von Wangelin, *Org. Biomol. Chem.*, 2010, **8**, 1695; (*c*) S. M. I. Al-Rafia, A. C. Malcolm, S. K. Liew, M. J. Ferguson, R. McDonald and E. Rivard, *Chem. Commun.*, 2011, **47**, 6987; (*d*) For an improved synthetic route to NHOs, see: K. Powers, C. Hering-Junghans, R. McDonald, M. J. Ferguson and E. Rivard, *Polyhedron*, 2016, DOI: 10.1016/j.poly.2015.07.070.

4 (*a*) A. C. Malcolm, K. J. Sabourin, R. McDonald, M. J. Ferguson and E. Rivard, *Inorg. Chem.*, 2012, **51**, 12905; (*b*) S. M. I. Al-Rafia, M. R. Momeni, M. J. Ferguson, R. McDonald, A. Brown and E. Rivard, *Angew. Chem., Int. Ed.*, 2013, **52**, 6390; (*c*) Y. Wang, M. Y. Abraham, R. J. Gilliard Jr., D. R. Sexton, P. Wei and G. H. Robinson, *Organometallics*, 2013, **32**, 6639; (*d*) R. S. Ghadwal, S. O. Reichmann, F. Engelhardt, D. M. Andrada and G. Frenking, *Chem. Commun.*, 2013, **49**, 9440; (*e*) S. M. I. Al-Rafia, M. R. Momeni, M. J. Ferguson, R. McDonald, A. Brown and E. Rivard, *Organometallics*, 2013, **32**, 6201; (*f*) S. Kronig, P. G. Jones and M. Tamm, *Eur. J. Inorg. Chem.*, 2013, 2301; (*g*) R. S. Ghadwal, C. J. Schürmann, F. Engelhardt and C. Steinmetzger, *Eur. J. Inorg. Chem.*, 2014, 4921; (*h*) R. S. Ghadwal, C. J. Schürmann, D. M. Andrada and G. Frenking, *Dalton Trans.*, 2015, **44**, 14359; (*i*) W.-H. Lee, Y.-F. Lin, G.-H. Lee, S.-M. Peng and C.-W. Chiu, *Dalton Trans.*, 2016, DOI: 10.1039/c5dt03847b.

5 For an important early study on the coordination of an NHO with Au(I) centers, see: A. Fürstner, M. Alcarazo, R. Goddard and C. W. Lehmann, *Angew. Chem., Int. Ed.*, 2008, **47**, 3210.

6 (*a*) R. D. Crocker and T. V. Nguyen, *Chem. – Eur. J.*, 2016, **22**, 2208; (*b*) S. Naumann, A. W. Thomas and A. P. Dove, *ACS Macro Lett.*, 2016, **5**, 134; (*c*) Y.-B. Wang, D.-S. Sun, H. Zhou, W.-Z. Zhang and X.-B. Lu, *Green Chem.*, 2015, **17**, 4009; (*d*) Y.-B. Jia, Y.-B. Wang, W.-M. Ren, T. Xu, J. Wang and X.-B. Lu, *Macromolecules*, 2014, **47**, 1966.

7 M. Iglesias, A. Iturmendi, P. J. Sanz Miguel, V. Polo, J. Pérez-Torrente and L. A. Oro, *Chem. Commun.*, 2015, **51**, 12431.

8 (*a*) A. Dumrath, X.-F. Wu, H. Neumann, A. Spannenberg, R. Jackstell and M. Beller, *Angew. Chem., Int. Ed.*, 2010, **49**, 8988; (*b*) A. Dumrath, C. Lübbe, H. Neumann, R. Jackstell and M. Beller, *Chem. – Eur. J.*, 2011, **17**, 9599.

9 S. M. I. Al-Rafia, M. J. Ferguson and E. Rivard, *Inorg. Chem.*, 2011, **50**, 10543.

10 F. H. Allen, O. Kennard, D. G. Watson, L. Brammer, A. G. Orpen and R. Taylor, *J. Chem. Soc., Perkin Trans. 2*, 1987, S1.

11 S. J. Berners-Price, L. A. Colquhoun, P. C. Healy, K. A. Byriel and J. V. Hanna, *J. Chem. Soc., Dalton Trans.*, 1992, 3357.

12 J. Schreiber, H. Maag, N. Hashimoto and A. Eschenmoser, *Angew. Chem., Int. Ed. Engl.*, 1971, **10**, 330.

13 J. Monot, M. Makhlouf Brahmi, S.-H. Ueng, C. Robert, M. Desage-El Murr, D. P. Curran, M. Malacria, L. Fensterbank and E. Lacôte, *Org. Lett.*, 2009, **11**, 4914.

14 H. Dorn, E. Vejzovic, A. J. Lough and I. Manners, *Inorg. Chem.*, 2001, **40**, 4327.

15 (*a*) C. W. Cheung, D. S. Surry and S. L. Buchwald, *Org. Lett.*, 2013, **15**, 3734; (*b*) J. D. Hicks, A. M. Hyde, A. M. Cuezva and S. L. Buchwald, *J. Am. Chem. Soc.*, 2009, **131**, 16720; (*c*) R. J. Lundgren, B. D. Peters, P. G. Alsabeh and M. Stradiotto, *Angew. Chem., Int. Ed.*, 2010, **49**, 4071; (*d*) S. M. Crawford, C. B. Lavery and M. Stradiotto, *Chem. – Eur. J.*, 2013, **19**, 16760.

16 (*a*) C. Valente, S. Çalimsiz, K. H. Hoi, D. Mallik, M. Sayah and M. G. Organ, *Angew. Chem., Int. Ed.*, 2012, **51**, 3314; (*b*) S. Meiries, G. Le Duc, A. Chartoire, A. Collado, K. Speck, K. S. A. Arachchige, A. M. Z. Slawin and S. P. Nolan, *Chem. – Eur. J.*, 2013, **19**, 17358.

17 W. A. Herrmann, M. Elison, J. Fischer, C. Köcher and G. R. J. Artus, *Angew. Chem., Int. Ed. Engl.*, 1995, **34**, 2371.

18 (*a*) A. R. Martin, A. Chartoire, A. M. Z. Slawin and S. P. Nolan, *Beilstein J. Org. Chem.*, 2012, **8**, 1637; (*b*) P. R. Melvin, D. Balcells, N. Hazari and A. Nova, *ACS Catal.*, 2015, **5**, 5596.

19 M. S. Viciu, O. Navarro, R. F. Germaneau, R. A. Kelly III, W. Sommer, N. Marion, E. D. Stevens, L. Cavallo and S. P. Nolan, *Organometallics*, 2004, **23**, 1629.

20 (*a*) A. S. K. Hashmi, *Angew. Chem., Int. Ed.*, 2005, **44**, 6990; (*b*) D. J. Gorin, B. D. Sherry and F. D. Toste, *Chem. Rev.*, 2008, **108**, 3351; (*c*) C. Obradors and A. M. Echavarren, *Acc. Chem. Res.*, 2014, **47**, 902; (*d*) H. Yang and F. P. Gabbaï, *J. Am. Chem. Soc.*, 2015, **137**, 13425.

21 P. Pérez-Galán, N. Delpont, E. Herrero-Gómez, F. Maseras and A. E. Echavarren, *Chem. – Eur. J.*, 2010, **16**, 5324.

22 (*a*) A. Sidiropoulos, C. Jones, A. Stasch, S. Klein and G. Frenking, *Angew. Chem., Int. Ed.*, 2009, **48**, 9701; (*b*) S. M. I. Al-Rafia, P. A. Lummis, A. K. Swarnakar, K. C. Deutsch, M. J. Ferguson, R. McDonald and E. Rivard, *Aust. J. Chem.*, 2013, **66**, 1235.

23 (*a*) H. K. Lenker, T. G. Gray and R. A. Stockland, *Dalton Trans.*, 2012, **41**, 13274; (*b*) S. G. Weber, D. Zahner, F. Rominger and B. F. Straub, *Chem. Commun.*, 2012, **48**, 11325; (*c*) N. Phillips, T. Dodson, R. Tirfoin, J. I. Bates and S. Aldridge, *Chem. – Eur. J.*, 2014, **20**, 16721.

24 A. B. Pangborn, M. A. Giardello, R. H. Grubbs, R. K. Rosen and F. J. Timmers, *Organometallics*, 1996, **15**, 1518.

25 L. S. Jafarpour, E. D. Stevens and S. P. Nolan, *J. Organomet. Chem.*, 2000, **606**, 49.

26 G. M. Sheldrick, *Acta Crystallogr., Sect. A: Found. Crystallogr.*, 2008, **64**, 112.

27 P. T. Beurskens, G. Beurskens, R. de Gelder, J. M. M. Smits, S. Garcia-Granda and R. O. Gould, *DIRDIF-2008 Program. Crystallographic Laboratory*, Radboud University, Nijmegen, The Netherlands.

28 (*a*) A. L. Spek, *Acta Crystallogr., Sect. C: Cryst. Struct. Commun.*, 2015, **71**, 9; (*b*) A. L. Spek, *PLATON - a multipurpose crystallographic tool*, Utrecht University, Utrecht, The Netherlands.

